

Synthesis, Structural and Mechanical Properties of $\text{Ni}_{1-x}\text{Cd}_x\text{Fe}_2\text{O}_4$ ferrites (X=0.1, 0.2, 0.3, and 0.4)

Pratibha Bakale¹, Pragati Guggari¹, Apeksha Keste¹, A.S.Pujar²,
S.N.Mathad^{3*}, C.S.Hiremath⁴, P.R.Jeergal¹, R.B.Pujar¹

¹ Department of Physics, P.C. Jabin Science College, Hubballi, Karnataka, 580031 India

² Department of Physics, K.L.E. Society's Raja Lakhamagouda Science Institute, Belagaum, Karnataka, 590001 India

³ Department of Physics, K.L.E. Institute of Technology, Hubli, Karnataka, 580030 India

⁴ S.K.Arts and H.S.K Science Institute, Hubballi, Karnataka, 580031 India

ABSTRACT: Study of nickel ferrite structure adding with cadmium (X=0.1, 0.2, 0.3, and 0.4) using standard ceramic method has been used to prepared the samples at 1000 °C for 15 hours. The pattern of X-ray diffraction of samples showed that has a single phase cubic spinel structure. The variation of lattice constant has been observed in the range 8.4511- 8.4707 Å and crystalline samples are ranging from 35 to 43 nm. The grain size was increases with increases the additives of cadmium through SEM analysis.

KEYWORDS: Ferrites, XRD, SEM, and FTIR

<https://doi.org/10.29294/IJASE.6.2.2019.1285-1290>

© 2019 Mahendrapublications.com, All rights reserved

1. INTRODUCTION

In recent days, nanocrystalline ferrites become a subject of fascination because of their overwhelming application in human life as well as research areas [1-3]. Ferrites are an important class of magnetic materials which have many applications, ranging from radio frequency to microwave frequency. They can be used in transformers, inductors, antenna rod, memory chip, and sensors [4-5]. Insulating magnetic oxides have, low eddy current, dielectric losses, high value of saturation magnetization, permeability, and moderate permittivity which are recognized by the chemical formula MFe_2O_4 , where 'M' stands for divalent metal ions. M can be replaced by other divalent metal ions and we can have number of spinel ferrites [6-7]. Because of high resistivity, low cost, easy for manufacture, superior over conventional magnetic material, there are used in radar, audio-video and digital recording, bubble devices, memory cores of computers, satellites communication and microwave devices [8-9]. The series $\text{Ni}_{1-x}\text{Zn}_x\text{Fe}_2\text{O}_4$, $\text{Cu}_{1-x}\text{Zn}_x\text{Fe}_2\text{O}_4$, $\text{Ni}_{0.8-x}\text{Cu}_x\text{Zn}_{0.2}\text{Fe}_2\text{O}_4$, of ferrites have been prepared using solid state method. $\text{Co}_{1-x}\text{Ni}_x\text{Fe}_2\text{O}_4$ Ferrites with (x=0.0,0.1,0.2,0.3,0.4,0.5), were prepared by Gul et al [10] by chemical co- precipitation method with grain size (14 to 21 nm) and resistivity increased from $1.98 \times 10^6 (\Omega\text{cm})$ to $8.323 \times 10^6 (\Omega\text{cm})$ at temperature 393K. Structural and electrical properties of $\text{Ni}_{1-x}\text{Mg}_x\text{Fe}_2\text{O}_4$ (x= 0.0, 0.3,0.6,0.9) synthesized by citrate gel process were discussed by Berchman et al [11] with increase in Mg concentration dielectric constant decreased with the rise in the frequency and AC conductivity increased with the rise in frequency. Measurement of exchange interaction in Ti-substituted Ni-ferrites prepared by

standard ceramic technique was reported by Islam et al.[12]. Effective magnetic moment and exchange interaction both decreased whereas Curie temperature increased with the increase in Ti concentration. The dielectric attributes of $\text{Mn}_x\text{Ni}_{0.5-x}\text{Zn}_{0.5}\text{Fe}_2\text{O}_4$ (x=0.05 to 0.4) synthesized by the citrate precursor method have been investigated as a function of frequency, temperature, composition, and sintering temperature by Singh et al.[13].

In the recent years, ferrites have been prepared in nano crystalline by several techniques. The properties of these nano sized ferrites are different from that of bulk ferrites and hence they find applications in the field of drug delivery, MRI, hyperthermia, sensors, catalyst etc [14]. The most commonly used methods are ceramic method [15] co-precipitation method [16] precursor method and microwave method [17] micro emulsion method [18] reverse Micelle technique [19] and auto combustion [20-21].

Nickel ferrites are found to be versatile magnetic materials owing to their electric and magnetic properties which can be altered by suitable dopant. The literature survey shows less information on cadmium doped nickel ferrites ($\text{Ni}_{1-x}\text{Cd}_x\text{Fe}_2\text{O}_4$ with X=0.1, 0.2, 0.3 and 0.4). Logical conclusion, it is proposed to empathize the study on ample physical properties of Ni-Cd ferrites. X-ray spectra to confirm the single phase cubic structure, quantitative element ensue by EDAX, morphological study of samples by SEM and FTIR spectra to identify the absorption bands.

2. EXPERIMENTAL METHODS

AR grade Nickel oxide, Cadmium oxide, and Ferric oxide in molar proportions and mixed thoroughly in

*Corresponding Author: physicssiddu@gmail.com

Received: 19.09.2019

Accepted: 18.10.2019

Published on: 30.11.2019

Pratibha Bakale et al,

acetone medium in agate mortar. The ferrites with the general chemical formula $Ni_{1-x}Cd_xFe_2O_4$ where $x=0.1, 0.2, 0.3$, and 0.4 were synthesized by ceramic method. Then ferrite samples were pre sintered at 800°C for 10 hours [15]. The pre sintered powders were subjected to milling process in acetone medium. One or two drops of PVA solution of 20% concentration was added as binder. All samples were pressed in to pellets of 1cm in diameter and 0.2cm in height by using a die by applying a pressure of about 5 tones/ square inch for 5 minutes. The pellets were subjected to final sintering at 1000°C for 15 hours with the help of alumina boat to enable the completion of solid state reaction [15]. All the samples were furnace cooled in air medium. The physical density of each sample was calculated by mass and dimensions data. The schematic diagram of proposed work is shown in Figure 1.

3. RESULTS AND DISCUSSIONS

3.1 XRD studies

XRD used to determine structure of a crystal, in which the crystalline atoms cause a beam of incident X- ray to diffract into many specific directions. The XRD pattern of cadmium doped Ni-ferrites were shown in Figure 2 with peaks (220), (311), (222), (400), (422), (511), and (440) respectively. The diffraction maxima from Bragg's law is prevailed by

$$2d_{hkl} \cdot \sin \theta = n\lambda \quad \text{.....(1)}$$

$$d = \frac{a}{(h^2 + k^2 + l^2)^{1/2}} \quad \text{..... (2)}$$

It can be seen that the diffraction peaks are either all even or all odd, which suggests a spinel phase (lattice parameter= $8.4511- 8.4707 \text{ \AA}$) for sample and thus validates the cubic structure. The detailed information of sample like lattice parameter (a), and interplanar distances (d) are tabulated in Table 1. Average Crystallite size (D) is calculated by Debye - Sherrer's formula [22]

$$D = \frac{0.9 \cdot \lambda}{\beta_D \cdot \cos \theta} \quad \text{..... (3)}$$

The distance between magnetic ions (hopping length) in A site (Tetrahedral) and B site (Octahedral) were calculated by using [15,20] the complying relations $\{(L_A \text{ and } L_B)\}$

$$L_A = \frac{a \times \sqrt{3}}{4} \quad \text{..... (4)}$$

$$L_B = \frac{a \times \sqrt{2}}{4} \quad \text{..... (5)}$$

$$\text{micro-strain}(\epsilon) = \frac{\beta \cos \theta}{4} \quad \text{..... (6)}$$

$$\text{Dislocation Density}(\rho_D) = \frac{1}{D^2} \quad \text{..... (7)}$$

The detailed crystal size (D), dislocation density (ρ), micro-strain(ϵ), and lattice constant (a) tabulated in Table.No.2.

The porosity plays enormously significant role in the microstructure of ferrites and calculated by the relation

$$P = (d_x - d_a) / d_x \times 100 \quad \text{----(8)}$$

Where d_x =x-ray density = $8M/Na^3$ ---- (9)

N =Avagadro's number = 6.0238×10^{23} atoms/mole,
a=lattice constant

The porosity is found to vary from 35 to 59 %, depending on method of preparation, purity of starting raw materials, sintering time and temperature.

3.2 SEM and EDAX Analysis

SEM micrographs of the samples are represented Figure 3 and reveals that grain size increases with increases in the Cd content, because ionic radius of Cd^{+2} is greater than that of Ni^{+2} and Fe^{+3} . It is also due to the presence of certain amount of metal ion vacancies caused by oxidation of suitable dopant. The exaggerated grain growth occurs due to rapid growth of few grains at the expense of their neighbors due to lack of homogeneity. Hence it can be concluded that diameter of the grain increases with decrease in porosity and under specific conditions exaggerated grain growth may occur. Depending upon the heat treatment, the grain size varies from 400nm to 1250nm.

In the present study, it is observed that all the samples show exaggerated grain growth. An energy dispersive X-ray spectroscopy (EDX) spectrum of Ni-Cd ferrites was shown in Figure 4. The EDX spectra show the presence of Ni, Cd, Fe and O elements without impurities in the ferrite samples. The atomic % of the elements analyzed from the EDX spectra are in good agreement with the expected composition of elements in the ferrite samples before the synthesis. The non appearance of any extra peaks in the XRD patterns and EDX spectra of ferrites confirms that there are no impurities in the system.

Table 1 Inter-planar distance (d) and Lattice parameter (a)

X=0.1			X=0.2			X=0.3			X=0.4		
2 θ	(hkl)	d cal	2 θ	(hkl)	d cal	2 θ	(hkl)	d cal	2 θ	(hkl)	d cal
29.82	220	2.9968	29.81	2.9889	220	22.7094	4.8905	111	29.8048	2.900	220
35.20	311	2.5481	35.18	2.5489	311	29.8204	2.9948	220	35.1668	2.5498	311
36.86	222	2.4396	36.96	2.4404	222	35.9012	2.5540	311	36.9405	2.4413	222
42.92	400	2.1127	43.018	2.1134	400	36.9012	2.4452	222	38.1159	2.4413	222
53.29	422	1.7251	56.705	1.6269	511	38.0185	2.4452	222	42.9406	2.1142	400
56.85	511	1.6264	62.334	1.4944	440	42.936	2.1176	400	56.7546	1.6275	511
62.47	440	1.4939	74.264	1.2892	533	56.6508	1.6301	511	62.3392	1.4950	440
74.54	533	1.2887							73.7254	1.2896	533
a=8.4511 Å ⁰			a=8.4707 Å ⁰			a=8.4539 Å ⁰			a=8.4570 Å ⁰		

Table 2 Crystal size (D), dislocation density (ρ) and micro-strain (ϵ), lattice constant (a)

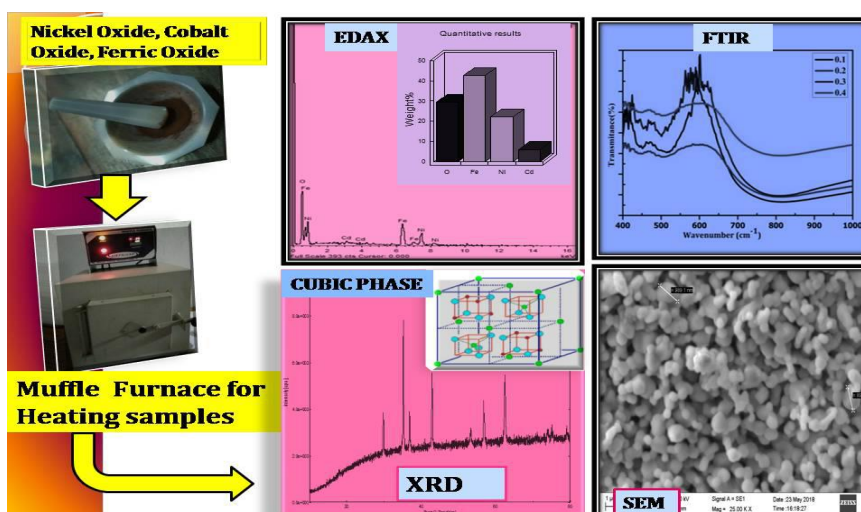
X	D=0.91 λ / β cos θ nm	$\rho = 1/D^2$	$\epsilon = \beta$ cos $\theta/4$	Lattice parameter (Å ⁰)	Hopping lengths (Å ⁰)	
					L _A	L _B
0.1	43.3	5.336×10 ¹⁴	0.8094×10 ⁻³	8.4511	3.659434	2.987915
0.2	35.12	8.1075×10 ¹⁴	0.9979×10 ⁻³	8.4539	3.660646	2.988905
0.3	38.35	6.7993×10 ¹⁴	0.9136×10 ⁻³	8.4707	3.667921	2.994845
0.4	37.03	7.292×10 ¹⁴	0.9463×10 ⁻³	8.4570	3.661988	2.990001

Table 3 Actual density, X-ray density, Porosity and grain size (SEM)

X	d _A gr/cc	d _x gr/cc	P=d _x -d _A /d _x ×100	Average grain diameter (From SEM) nm
0.1	3.384	5.276	35.859	400
0.2	3.105	5.265	41.625	900
0.3	3.055	5.474	44.190	1250
0.4	2.3471	5.618	58.77	650

Table 4 EDAX analysis (Atomic percentage of elements)

X	Ni	Cd	Fe	O	Total
0.1	20.56	0.35	22.68	56.41	100
0.2	11.96	0.73	26.07	61.25	100
0.3	12.84	1.61	24.27	61.28	100
0.4	12.35	1.74	25.17	60.74	100

**Figure 1 Schematic synthesis route of Ni-Cd ferrite.**

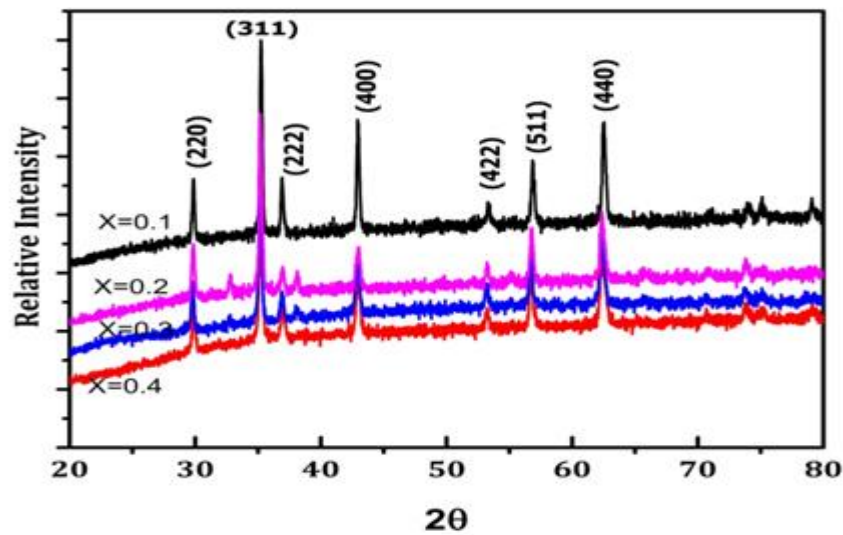


Fig.2 XRD patterns of Ni-Cd ferrites

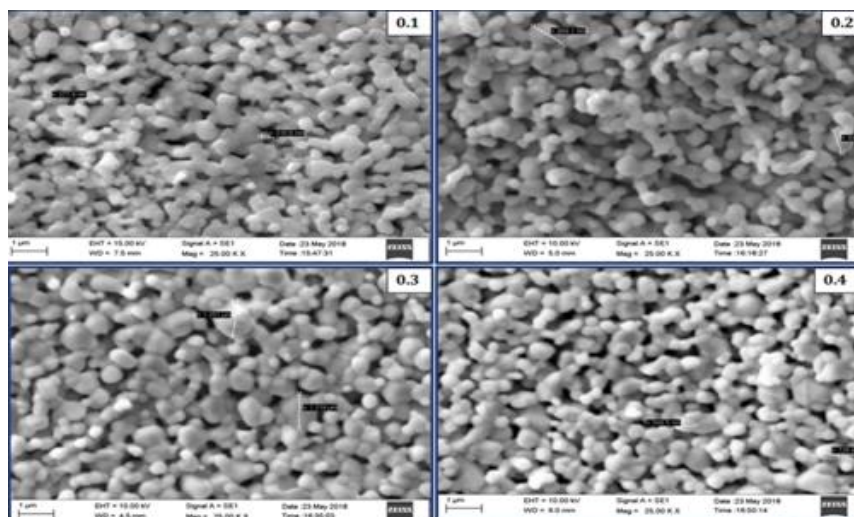


Figure 3 SEM images of Ni-Cd ferrite system

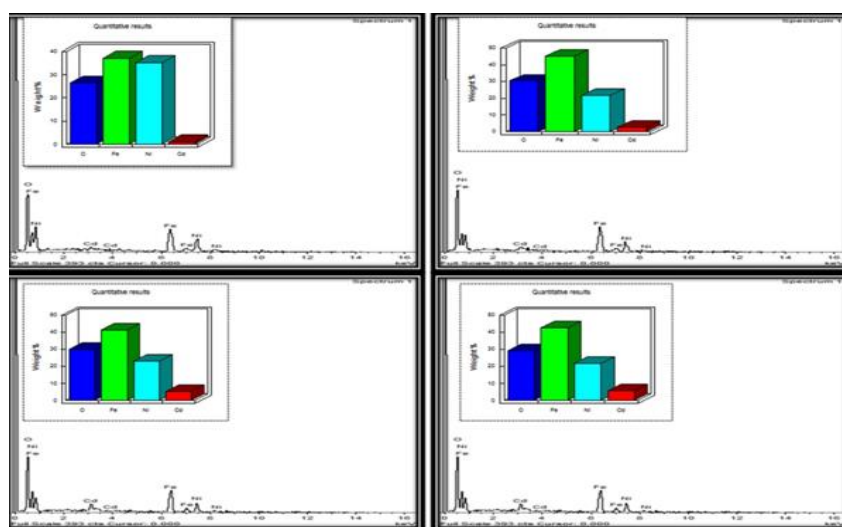


Figure 4 EDAX spectra of Ni-Cd ferrite system

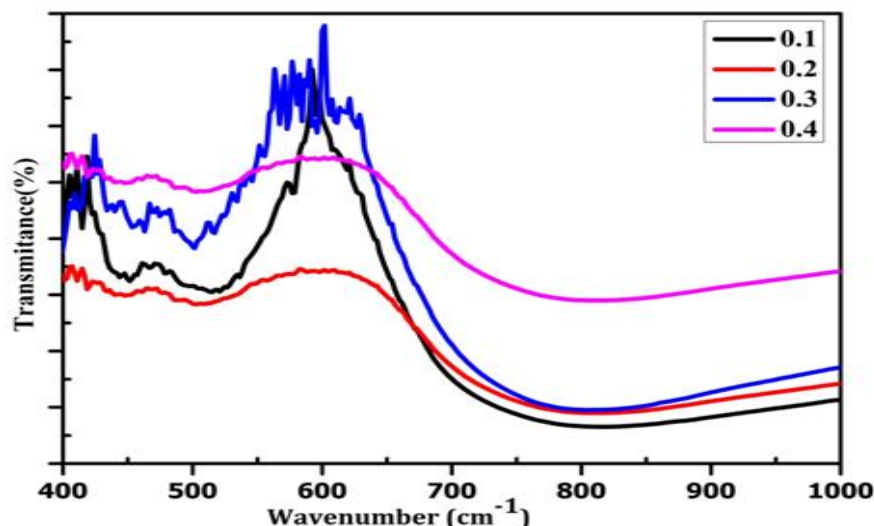


Figure 5 FTIR spectra of Ni-Cd ferrite system

3.3 FTIR Spectra

FTIR Spectra of the samples were obtained from in the range of 400cm^{-1} to 1000cm^{-1} is shown in Figure 5. The IR spectrum reveals two prominent bands near 600 cm^{-1} and 400 cm^{-1} which are assigned to tetrahedral and octahedral complexes respectively. Waldorn [24] assigned the absorption bands around 600cm^{-1} to the intrinsic vibrations of tetrahedral complexes corresponding to the highest restoring force where as the absorption bands around 400cm^{-1} assigned to intrinsic vibrations of octahedral complexes which are bond bending vibrations. In the present study the samples show prominent bands ν_1 and ν_2 around 600cm^{-1} and 400cm^{-1} respectively in agreement with Waldron assignment. The splitting of absorption bands around 400cm^{-1} is assigned to octahedral complexes which suggest the occupancy of B-sites by Cd ions. Similar results were in ferrites and appearance of IR absorption bands was reported in [24-26].

4. CONCLUSION

The structural, mechanical strain and morphological studies with cadmium doping of Ni-ferrite is studied which is synthesized by solid state method. The XRD study confirmed the formation of the single cubic phase; with lattice constant $8.4511\text{-}8.4707\text{\AA}$ and particle size is $35\text{-}43\text{ nm}$. The study of Fourier Transform Infrared Spectroscopy confirms the formation of spinel structure ferrite samples. SEM analysis grain size increases with increases in the Cd content.

REFERENCES

- [1]. Goldman, A., 2006, Modern Ferrite Technology, New York: Springer, 2006. book/9780387281513
- [2]. Maaz, K.; Mumtaz, Arif; Hasanain, S. K.; Ceylan, Abdullah, Synthesis and magnetic properties of cobalt ferrite (CoFe_2O_4) nanoparticles prepared by wet chemical route, Journal of Magnetism and Magnetic Materials, 308(2) 289-295, 2007
- [3]. Yakubu, A., Abbas, Z., Ibrahim, N. A., and Hashim, M., Effect of temperature on structural, magnetic and dielectric properties of cobalt ferrite nanoparticles prepared via co-precipitation method, Phys. Sci. Int. Journal, 8(1), 1-8, 2015
- [4]. N. Tran, T.J. Webster, 2010. Magnetic nanoparticles: biomedical applications and challenges, J. Mater. Chem. 20, 8760-8767.
- [5]. Zhao, L.J., Jianj, Q. 2010. Effects of applied magnetic field and pressures on the magnetic properties of nanocrystalline CoFe_2O_4 ferrite, J. Magn. Magn. Mater. 322, 2485
- [6]. Arruebo, M., Fernandez-P, R. M.R. Ibarra, J. Santamaria, 2007. Magnetic nanoparticles for drug delivery, Nano Today 2 (3) 22-32.
- [7]. Mammo, T.W., Murali, N., Sileshi, Y.M., T. Arunamani, 2017. Studies of structural, morphological, electrical, and magnetic properties of Mg substituted Co-ferrite materials synthesized using sol-gel autocombustion method, Phys. B: Condens. Matter 523, 24-30
- [8]. Haque, M.M., M.Huq, M.A. Hakim, 2009. Effect of Zn^{2+} substitution on the magnetic properties of $\text{Mg}_{1-x}\text{Zn}_x\text{Fe}_2\text{O}_4$ ferrites, Physica B 404, 3915.
- [9]. Rendale, M.K., Mathad, S.N., Puri, V., Resonance Shifting by Ferrite Thick film Superstrate, Serbian Journal of Electrical Engineering, Vol. 15, No. 3, October 2018, 275-284
- [10]. Gul, I.H., Amin, F, Abbasi, A.Z., M. Anis-ur-Rehman, Maqsood, A, 2007, Physical and magnetic characterization of co-precipitated nanosize Co-Ni ferrites, Scrip. Mater. 56, 497-500
- [11]. Berchmans, L.J., Selvan, R.K, Kumar, P.N.S. Augustin, C.O, 2007. Structural and electrical properties of $\text{Ni}_{1-x}\text{Mg}_x\text{Fe}_2\text{O}_4$

- synthesized by citrate gel process, J.Magn.Magn.Mater.279, 103-110
- [12]. Islam, M.U, Hashmi, K.A.,Rana, M.U, T.Abbas,2002. Measurement of exchange interaction in Ti-substituted Ni-ferrites, Solid State commun.121,51-54
- [13]. Singh, A.K., Goel, T.C.,Mendiratta, R. G,2002. Dielectric properties of Mn-substituted Ni-Zn ferrites, J.Appl.Phys.91,6626-6629
- [14]. Thakur A. and Singh, M. 2003, Preparation and characterization of nanosize Mn_{0.4}Zn_{0.6}Fe₂O₄ ferrite by citrate precursor method, Ceram. Int. 29, 505.
- [15]. Galagali, S.L. Patil, R.A. Adaki, R.B., Hiremath, C.S, Mathad, S.N., Pujar, R.B. 2018. Influence of Cadmium substitution in magnesium ferrites on Structural and Mechanical properties, Science of Sintering, 50, 217-223
- [16]. Yattinahalli, S.S., Kapatkar, S.B., Ayachit, N.H., and Mathad, S.N., 2013. Synthesis and structural characterization of nanosized nickel ferrite, Int. J. Self-Propag. High-Temp. Synth., 22, (3) 147-150.
- [17]. Molakeri, A. S., Kalyane, S., Mathad, S.N., 2017. Elastic Properties of nickel ferrite synthesized by combustion and microwave method using FT-IR spectra, International Journal of Advanced Science and Engineering, 3 (4) 422-427.
- [18]. Mathew, D.S. and Juang, R.-S., 2007, Structure and magnetism of spinel ferrite nanoparticles and their synthesis in microemulsions, J. Cheminf., 38(34), 1522- 2667.
- [19]. Kale, A., Gubbala, S., and Misra, R.D.K., 2004, Magnetic behavior of nanocrystalline nickel ferrite synthesized by the reverse micelle technique, J. Magn. Magn. Mater., 277, 350-358.
- [20]. Pathan, A.T., Mathad, S.N., and Shaikh, A.M., 2014. Infrared spectral studies of Co²⁺ substituted Li-NiZn nanostructured ferrites, Int. J. Self-Propag. High-Temp. Synth., 23(2) 112-117.
- [21]. Cyril Osereme E.E., Iserom, I. B., I. E. Eze Joshua, 2016. Synthesis, Microstructure and Magnetic Properties of Nano-crystalline MgFe₂O₄ Particles: Effect of Mixture of Fuels and Sintering Temperature, Science of Sintering, 48. 221-235
- [22]. Mathad, S.N., 2018. Mechanical and Structural Properties of Zn_{0.1}Ni_{0.4}Cu_{0.5}Fe₂O₄ Ferrite, Int. J. Adv. Sci. Eng. 5(2) 911-916.
- [23]. Waldron, R. D., 1953. Infrared spectra of ferrites, Phys. Rev., 99(6) 1727-1735.
- [24]. Reddy, P.V. and Reddy, V.D.J., 1994. Far infrared spectral studies of some lithium nickel mixed ferrites, Magn. Magn. Mater., 136(3) 279-283.
- [25]. Khemalapure, S. S., Hosamani, P. L., Mathad, S. N., Pujar, A. S., Hiremath, C. S., Pundalik R. Jeeragal, Pawar, S. S., Pujar, R. B., 2019. Synthesis, Structural and Dielectric Properties of Ni-Zn-Cu Ferrites, Advanced Science, Engineering and Medicine, 11(1-8).
- [26]. Pujar, A. S, Kulkarni, A.B., Mathad, S. N., Hiremath, C.S, Rendale, M.K., Patil, M.R, Pujar, R.B., 2018. Synthesis, Structural, FTIR and Electrical properties of CuxCo_{1-x}Fe₂O₄ (x= 0,0.4,1) Prepared by Solid State Method, International Journal of self propagating high temperature synthesis, 27(3) 174-179.